Supporting Information

Multi-walled carbon nanotubes modified $NiCo_2S_4$ for efficient photocatalytic reduction of hexavalent chromium

Qiu Jin[a], *Ziye Zheng*[a], *Yuxiao Feng*[a], *Tian Shuang*[a], *Zuoli He*[a,*]

[a] *Shandong Key Laboratory of Water Pollution Control and Resource Reuse, School of Environmental Science and Engineering, Shandong University, Qingdao 266237, China;*

*Corresponding author: *Zuoli He*;

Email address: zlhe@sdu.edu.cn(Z. He)

Materials

PVP (K30), multi-walled carbon nanotubes (MWCNTs), nickel chloride hexahydrate ($NiCl_2 \cdot 6H_2O$), cobalt chloride hexahydrate ($CoCl_2 \cdot 6H_2O$), urea, sodium sulfide nonahydrate ($Na_2S \cdot 9H_2O$), $C_{13}H_{14}N_4O$ (DPC), potassium dichromate ($K_2Cr_2O_7$), H_2SO_4 were purchased from Aladdin Inc. (Shanghai, China). The ultrapure water (UPW) used in all experiments was obtained from a Direct-Q system (Millipore, Billerica, MA) with a resistivity of 18.2 MΩ/cm.

Characterizations

The crystal structure of the samples was determined via Bruker D8 X-ray diffractometer (XRD) using Cu target radiation source (λ = 0.154178 nm). Transmission electron micrographs (TEM) and high-resolution transmission electron microscopy (HRTEM) images were obtained by using a Talos F200X transmission electron microscope (FEI, USA). X-ray photoelectron spectroscopy (XPS) measurements were conducted by using Thermo Scientific K-Alpha+ with a mono-chromic X-ray source (Al Kα line, 1486.6 eV). UV-vis diffuse reflection spectra (UV-vis DRS) were carried by (UV2600). The 300 W Xenon lamp (CEL-HXF300-T3) worked as a UV-vis light source.

Electrochemical Measurements

Electrochemical analysis was carried out via an electrochemical workstation (660E). The test system employed a standard three-electrode system containing a Pt foil counter electrode, Ag/AgCl reference electrode and a working electrode. The working electrode was prepared as follows: 10 mg samples and 10 μL Nafion aqueous were added to 1 mL ethanol, then sonicated for 30 min to get a slurry mixture. Part of the mixture (40 μL) was dropped onto the 1×2 cm^2 FTO glass and dried at room temperature overnight. The

electrolyte was chosen as 0.1 M Na_2SO_4 aqueous solution and transient photocurrent, EIS responses were conducted under intermittent simulated solar light, and the light source was a 300 W Xe lamp (CEL-HXF300-T3). Mott-Schottky plots of the photocatalysts were collected at 1000 Hz with a potential range of -1 V to 1 V.

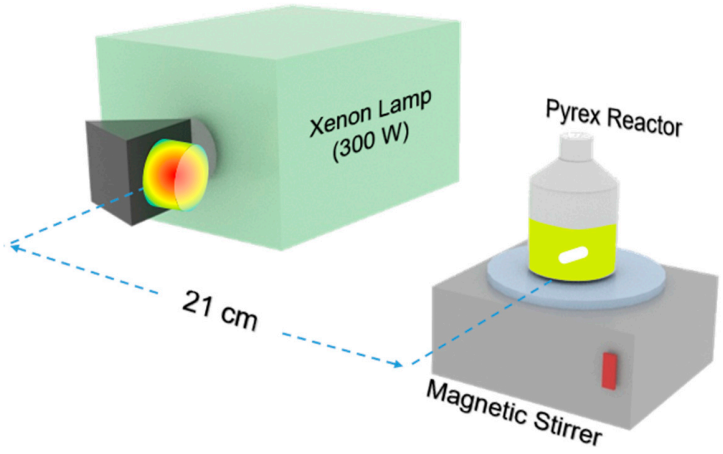

Figure S1. The schematic diagram of the reactor.

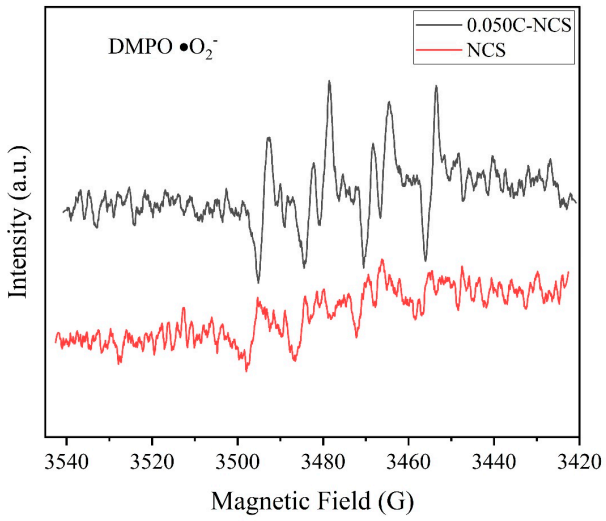

Figure S2. ESR spectrum of the $\bullet O_2^-$ produced by $NiCo_2S_4$ and 0.050 CNT-$NiCo_2S_4$ under visible-light irradiation.

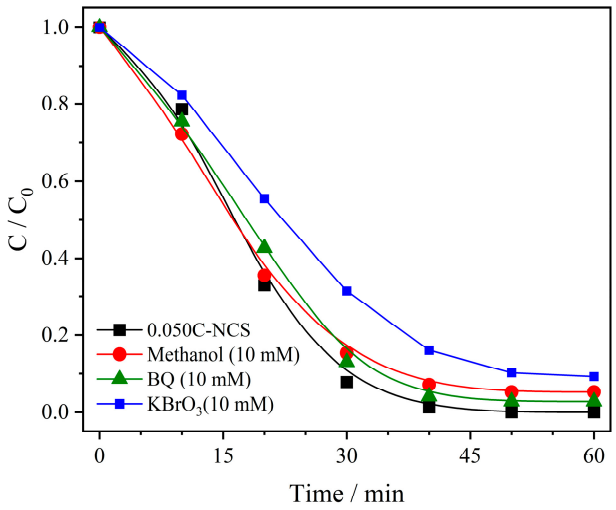

Figure S3. Effect of scavengers on photocatalytic degradation of Cr(VI) during the trapping experiments of the 0.050 CNT-$NiCo_2S_4$.

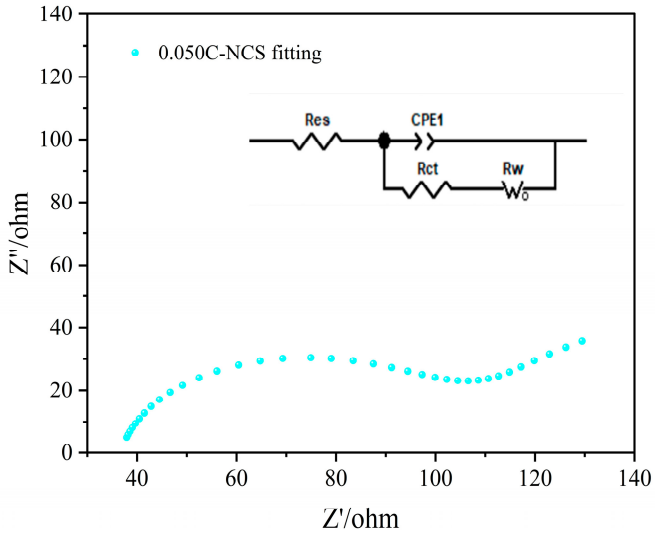

Figure S4. Circuit fitted Nyquist plot of the 0.050C-NCS with a suitable modified Randle circuit (inset).

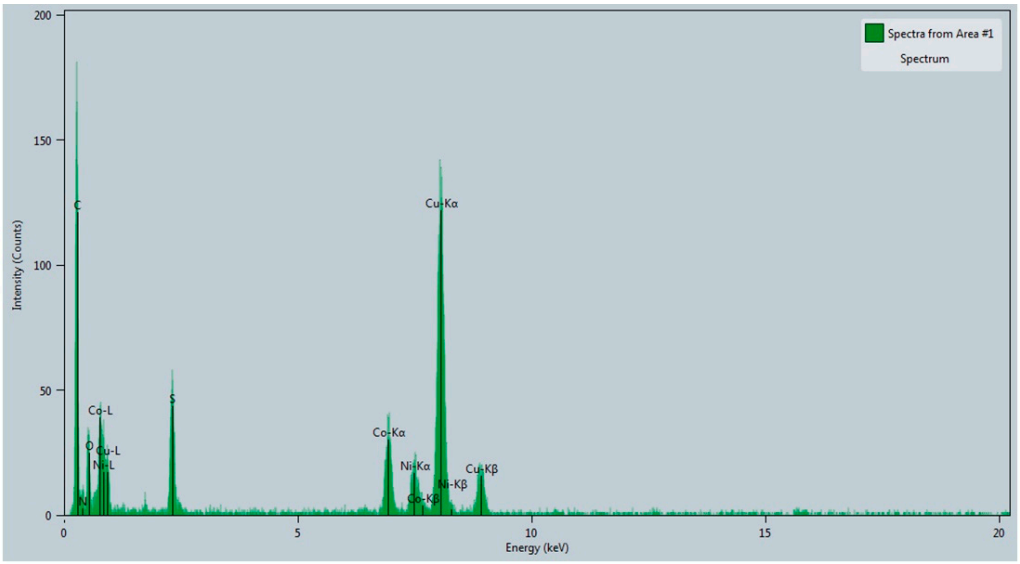

Figure S5. Energy dispersive spectroscopy of 0.050 CNT-$NiCo_2S_4$.

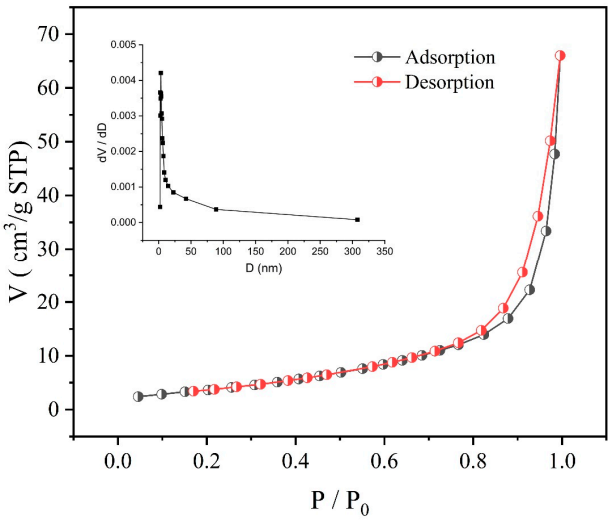

Figure S6. N_2 adsorption and desorption isotherms and corresponding pore-size distribution curves (inset) for 0.005 CNT-$NiCo_2S_4$.

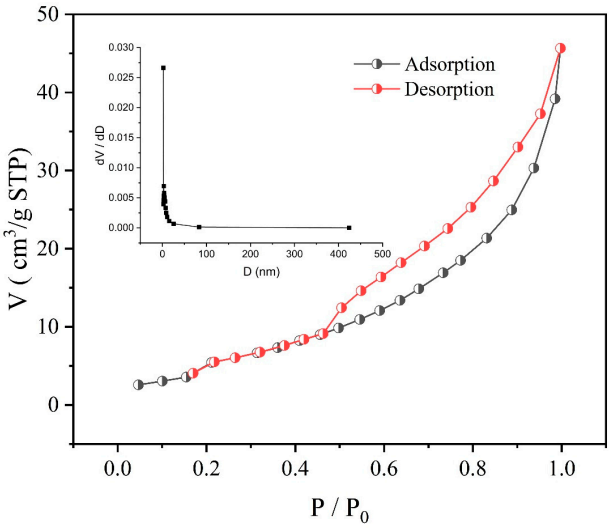

Figure S7. N_2 adsorption and desorption isotherms and corresponding pore-size distribution curves (inset) for 0.035 CNT-$NiCo_2S_4$.

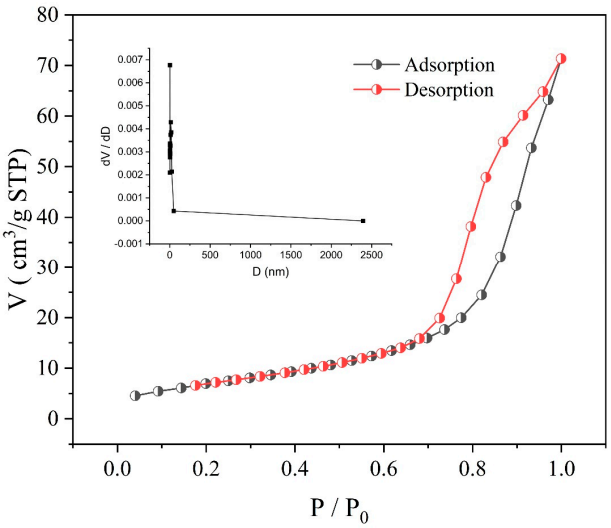

Figure S8. N_2 adsorption and desorption isotherms and corresponding pore-size distribution curves (inset) for 0.075 CNT-$NiCo_2S_4$.

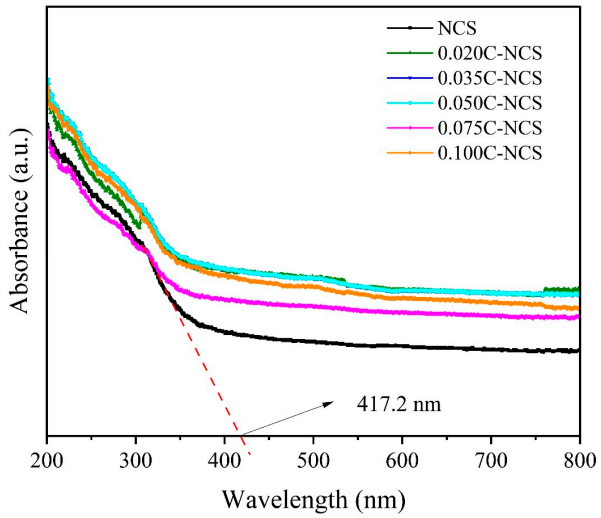

Figure S9. UV–vis Diffuse Reflectance Absorption Spectra (DRS) of as-prepared samples with different amounts of CNT

Table S1. Comparison of photocatalytic efficiency for photocatalytic reduction of Cr(VI) between previously reported literature and the present work.

Material	**$C_{catalyst}$ (g/L)**	**$C_{Cr(VI)}$ (mg/L)**	**Reaction Time Adsorption + catalytic (min)**	**Removal (%)**	**Refs.**
OH-TiO_2	1	10	30 min + 30 min	88	[1]
TiO_2/Nd	1	10	30 min + 180 min	99	[2]
$Gd(OH)_3$/RGO	1	10	30 min + 120 min	83	[3]
RGO/αFeOOH	1	10	30 min + 180 min	94	[4]
$SrTiO_3$	1	20	60 min + 240 min	99	[5]
$ZnWO_4$	1	40	60 min + 45 min	32	[6]
ZrO_2-CuO	1	40	10 min + 20 min	80	[7]
rGO@TiO_2	0.67	10	30 min + 180 min	98	[8]
$BiVO_4$/Bi_2S_3	0.5	10	10 min + 60 min	91.2	[9]
Bi_2S_3	0.5	40	30 min + 120 min	90	[10]
SnO_2@Bi_2WO_6	0.3	10	15 min + 50 min	98.2	[11]
MoS_2-Bi_2S_3	0.25	5	60 min + 30 min	98	[12]
CPVA/MoS_2-OH	0.2	100	60 min + 105 min	96	[13]
Bi_2MoO_6/Bi_2S_3	0.4	20	80 min + 16 min	100	[14]
BiOCl/Bi_2S_3	1	50	40 min + 9 min	100	[15]
SnS_2-In_2S_3	0.2	40	30 min + 30 min	100	[16]
0.050C-NCS	0.5	50	30 min + 40 min	100	Here

[1] Y. Li, Y. Bian, H. Qin, Y. Zhang, Z. Bian, Photocatalytic reduction behavior of hexavalent chromium on hydroxyl modified titanium dioxide, Appl. Catal. B, 206 (2017) 293-299.
[2] S. Rengaraj, S. Venkataraj, J.-W. Yeon, Y. Kim, X.Z. Li, G.K.H. Pang, Preparation, characterization and application of Nd-TiO_2 photocatalyst for the reduction of Cr(VI) under UV light illumination, Appl. Catal. B, 77 (2007) 157-165.
[3] D.K. Padhi, G.K. Pradhan, K.M. Parida, S.K. Singh, Facile fabrication of $GdOH_3$ nanorod/RGO composite: Synthesis, characterisation and photocatalytic reduction of Cr(VI), Chem. Eng. J., 255 (2014) 78-88.
[4] D.K. Padhi, K. Parida, Facile fabrication of alpha-FeOOH nanorod/RGO composite: A robust photocatalyst for reduction of Cr(VI) under visible light irradiation, J. Mater. Chem. A, 2 (2014) 10300-10312.
[5] D. Yang, Y. Sun, Z. Tong, Y. Nan, Z. Jiang, Fabrication of bimodal-pore $SrTiO_3$ microspheres with excellent photocatalytic performance for Cr(VI) reduction under simulated sunlight, J. Hazard. Mater., 312 (2016) 45-54.
[6] H. He, Z. Luo, Z.-Y. Tang, C. Yu, Controllable construction of $ZnWO_4$ nanostructure with enhanced performance for photosensitized Cr(VI) reduction, Appl. Surf. Sci., 490 (2019) 460-468.
[7] B. Nanda, A.C. Pradhan, K.M. Parida, Fabrication of mesoporous CuO/ZrO_2-MCM-41 nanocomposites for photocatalytic reduction of Cr(VI), Chem. Eng. J., 316 (2017) 1122-1135.
[8] L. Liu, C. Luo, J. Xiong, Z. Yang, Y. Zhang, Y. Cai, H. Gu, Reduced graphene oxide (rGO) decorated TiO_2 microspheres for visible-light photocatalytic reduction of Cr(VI), J Alloy Compd, 690 (2017) 771-776.
[9] X. Gao, H.B. Wu, L. Zheng, Y. Zhong, Y. Hu, X.W. Lou, Formation of mesoporous heterostructured $BiVO_4$/Bi_2S_3 hollow discoids with enhanced photoactivity, Angew. Chem. Int. Ed., 53 (2014) 5917-5921.
[10] S. Luo, F. Qin, Y.a. Ming, H. Zhao, Y. Liu, R. Chen, Fabrication uniform hollow Bi_2S_3 nanospheres via Kirkendall effect for photocatalytic reduction of Cr(VI) in electroplating industry wastewater, J. Hazard. Mater., 340 (2017) 253-262.
[11] N. Song, M. Zhang, H. Zhou, C. Li, G. Liu, S. Zhong, S. Zhang, Synthesis and properties of Bi_2WO_6 coupled with SnO_2 nano-microspheres for improved photocatalytic reduction of Cr^{6+} under visible light irradiation, Appl. Surf. Sci., 495 (2019) 143551.
[12] B. Weng, X. Zhang, N. Zhang, Z.-R. Tang, Y.-J. Xu, Two-dimensional MoS_2 nanosheet-coated Bi_2S_3 discoids: Synthesis, formation mechanism, and photocatalytic application, Langmuir, 31 (2015) 4314-4322.
[13] K. Wang, P. Chen, W. Nie, Y. Xu, Y. Zhou, Improved photocatalytic reduction of Cr(VI) by molybdenum disulfide modified with conjugated polyvinyl alcohol, Chem. Eng. J., 359 (2019) 1205-1214.
[14] X.-Q. Qiao, Z.-W. Zhang, Q.-H. Li, D. Hou, Q. Zhang, J. Zhang, D.-S. Li, P. Feng, X. Bu, In situ synthesis of n-n Bi_2MoO_6 & Bi_2S_3 heterojunctions for highly efficient photocatalytic removal of Cr(Ⅵ), J. Mater. Chem. A, 6 (2018) 22580-22589.
[15] Y. Lu, J. Song, W. Li, Y. Pan, H. Fang, X. Wang, G. Hu, Preparation of BiOCl/Bi_2S_3 composites by simple ion exchange method for highly efficient photocatalytic reduction of Cr^{6+}, Appl. Surf. Sci., 506 (2020) 145000.
[16] L. Wang, S.K. Karuturi, L. Zan, SnS_2-In_2S_3 p-n heterostructures with enhanced Cr^{6+} reduction under visible-light irradiation, Appl. Surf. Sci., 537 (2021) 148063.